HAL
open science

Methylcyclohexane pyrolysis and oxidation in a jet-stirred reactor

Tony Bissoonauth, Zhandong Wang, Samah y Mohamed, Jui-Yang Wang, Bingjie Chen, Anne Rodriguez, Ophélie Frottier, Xiaoyuan Zhang, Yan Zhang, Chuangchuang Cao, et al.

To cite this version:

Tony Bissoonauth, Zhandong Wang, Samah y Mohamed, Jui-Yang Wang, Bingjie Chen, et al.. Methylcyclohexane pyrolysis and oxidation in a jet-stirred reactor. Proceedings of the Combustion Institute, 2018, 37, pp.409-417. 10.1016/j.proci.2018.05.086 . hal-01922891

HAL Id: hal-01922891

https://hal.science/hal-01922891v1

Submitted on 14 Nov 2018

HAL is a multi-disciplinary open access archive for the deposit and dissemination of scientific research documents, whether they are published or not. The documents may come from teaching and research institutions in France or abroad, or from public or private research centers.

L'archive ouverte pluridisciplinaire **HAL**, est destinée au dépôt et à la diffusion de documents scientifiques de niveau recherche, publiés ou non, émanant des établissements d'enseignement et de recherche français ou étrangers, des laboratoires publics ou privés.

Methylcyclohexane pyrolysis and oxidation in a jet-stirred reactor

Tony Bissoonauth[a], Zhandong Wang[a], Samah Y. Mohamed[a], Jui-yang Wang[a], Bingjie Chen[a], AnneRodriguez[b], Ophélie Frottier[b], Xiaoyuan Zhang[c], Yan Zhang[c], Chuangchuang Cao[c], Juizhong Yang[c], Olivier Herbinet[b], Frédérique Battin-Leclerc[b], S. Mani Sarathy[a]

[a] *King Abdullah University of Science and Technology (KAUST), Clean Combustion Research Center (CCRC), Thuwal 23955-6900, Saudi Arabia*
[b] *Laboratoire Réactions et Génie des Procédés, CNRS, Université de Lorraine, ENSIC, 1, rue Grandville, BP 20451, 54001 Nancy Cedex, France*
[c] *National Synchrotron Radiation Laboratory, University of Science and Technology of China, Hefei, Anhui 230029, PR China*

Published in Proceedings of the Combustion Institute
https://doi.org/10.1016/j.proci.2018.05.086

Abstract

Alkylated cycloalkanes are an important chemical class in conventional fuels. Methylcyclohexane (MCH) is a simple alkylated cycloalkane that is a potential candidate to represent the naphthenic content in transportation fuel surrogates. Detailed experimental speciation data for MCH gas-phase oxidation and pyrolysis is still lacking in the literature. This work investigates the high-temperature pyrolysis and low-temperature oxidation of MCH in a jet-stirred reactor. Under low-temperature conditions, highly oxygenated intermediate species indicative of "alternative isomerization" of hydroperoxyalkylperoxy (OOQOOH) radicals and the subsequent third sequential O_2 addition are presented. Furthermore, a detailed chemical kinetic model capable of predicting MCH combustion was developed using new thermodynamic group values and recently published rate coefficients. Alternative isomerization of OOQOOH radicals and third sequential O_2 addition pathways were incorporated into the reaction mechanism. Additionally, an approach for reducing the complexity of the MCH low-temperature chemical pathways has been investigated to limit the arduousness of developing kinetic models. The experimentally measured species concentration profiles at atmospheric pressure, equivalence ratios of 0.25, 1.0, 2, and ∞, and temperatures in the range of 500–1100 K were used to validate and improve the chemical kinetic model. The model was further tested against rapid compression machine ignition delay times taken from literature.

Keywords: Low-temperature oxidation; Peroxides; Kinetic modeling; Synchrotron VUV photoionization mass spectrometry; Ignition delay time

Corresponding author : Zhandong Wang
zhandong.wang@kaust.edu.sa

1. Introduction

Emerging combustion modes in internal combustion engines, such as Homogeneous Charge Compression Ignition (HCCI), promise a reduction in the emission of harmful pollutants. Combustion phasing for this combustion mode is dominated by the chemical reaction kinetics of the fuel; its auto ignition plays a particularly significant role in controlling the performance and emissions [1]. Thus, there is a continued interest in developing accurate and detailed kinetic models for fuel oxidation chemistry.

Cycloalkanes (naphthenes) are an important class of compounds in transportation fuels [2,3]. They make a significant fraction of practical fuels, including jet fuels (~20%), gasoline (~10%), and depending on the crude source and degree of hydro processing, may constitute one-third or more by weight of diesel fuels [4]. Naphthenes play an important role in the formation of aromatic pollutants and polycyclic aromatic soot precursors [5]. Gasoline fuels typically contain significant amounts of C_5-C_7 cycloalkanes, such as cyclopentane [6,7], methylcyclopentane, cyclohexane [8] and methyl and ethylcyclohexane [9,10]. Amongst these, MCH is a simple alkylated cycloalkane frequently suggested as a candidate surrogate to represent the naphthenic content in transportation fuels [2,3].

Various fundamental studies have been conducted for MCH gas-phase reactions, such as experimental measurements of its pyrolysis [9,11], laminar premixed flame speciation profiles [9,12], ignition delay times [13,14], and laminar flame speeds [15]; reduced, skeletal, and detailed kinetic modeling of MCH combustion [9,13,16,17]; and theoretical calculations of important reaction pathways [9,18-20]. Details of published studies about MCH can be found in the papers of Wang et al. [9] and Narayanaswamy et al. [17].

The motivation of the present work is to (1) measure the detailed speciation products of MCH low- and high-temperature oxidation, and pyrolysis in a jet-stirred reactor (JSR). The literature lacks experimental speciation data for the low-temperature oxidation chemistry of MCH. Gas Chromatography (GC) was used to measure the stable oxidation intermediates. In addition, synchrotron vacuum ultraviolet photoionization molecular beam mass spectrometry (SVUV-PI-MBMS), which has been widely used in combustion studies [21-25], was used to detect the peroxide species in MCH oxidation. Such data is lacking in literature, and is needed to understand MCH reaction pathways and test kinetic models. The JSR pyrolysis data measured in this work by GC complements previous flow reactor data [9] measured by SVUV-PI-MBMS. Both data are adopted to validate the kinetic model in this work; and (2) develop a preliminary kinetic model of MCH oxidation. The rate constants for some key reactions, e.g., R + O_2 reaction network, were taken from recent quantum chemistry calculations [19,20,26]. Additional reaction classes such as the "alternative isomerization" of OOQOOH to $P(OOH)_2$ radical and subsequent reactions of $P(OOH)_2$ radical including a third sequential O_2 addition reaction network [27,28] were also included. In addition, the thermodynamic data was updated by using new group values from Burke et al. [29] in the calculation of Benson's group additivity. Furthermore, a step-wise method, grounded in "chemical knowledge", for reducing the number of reactions and species was investigated during the kinetic model development. The kinetic model was tested using the JSR pyrolysis and oxidation data obtained in this work, as well as ignition delay times taken from literature [13,14]. The discussion focuses on the low-temperature oxidation kinetics of MCH and the methodology behind developing the kinetic model.

2. Experimental methods

Pyrolysis and oxidation of MCH at atmospheric pressure were studied in three fused silica JSRs using different analytical tools. The three experiments are complementary, i.e., KAUST JSR-1 coupled with an Agilent refinery gas analyzer (RGA) can measure pyrolysis products, Nancy JSR-2 coupled with three GCs provides data of stable oxidation products, and Hefei JSR-3 with SVUV-PI-MBMS can measure highly reactive peroxide intermediates. Details of the three JSRs and the experimental procedures can be found in literature [25,30,31].

MCH pyrolysis was studied in JSR-1 (volume of 76 cm^3) with N_2 as the dilution gas. A residence time of 1 s was chosen and the initial mole fraction of MCH was kept at 1000 ppm to reduce coking in the JSR at high temperature. After pyrolysis, further gas reactions were frozen by a pressure-drop in the sonic-throat gas sampling, then the sample gas was analyzed online using Agilent RGA and Agilent 7890B GC. The RGA system, following ASTM D1945, D1946, and UOP 539 methods, was used to quantify H_2, methane, acetylene, ethylene, ethane, propene, 1,3-butadiene. The Agilent 7890B system was equipped with a DB-1 column to measure MCH. The uncertainty on reactants is ± 5%, whilst for the pyrolysis products is estimated to be around ± 15%.

For the Nancy experiment, MCH oxidation at three equivalences (i.e., 0.25, 1.0, and 2.0) was investigated from 500 to 1100 K with helium as the dilution gas. The initial MCH mole fraction for the three experiments was kept at ~ 5700 ppm. The oxidation products were analyzed online by three GCs equipped with different columns (i.e., carbosphere packed column, PlotQ capillary column, HP-5 capillary column) and detectors (thermal conductivity detector, flame ionization detector, and mass spectrometer), to measure C_1–C_4 hydrocarbons, small oxygenated compounds, as well as hydrocarbons and oxygenated species with more than five heavy atoms (i.e., carbon and oxygen atoms), and to identify the structure of unknown intermediates. Calibration was performed by injecting known amounts of pure substances when available; otherwise, the method of the effective carbon number was adopted. The uncertainty of the species mole fractions was about ± 5% with online analysis of reactants and C_1–C_2 hydrocarbons, and about ± 10% for analysis of other species.

In the Hefei experiment, the JSR was coupled with SVUV-PI-MBMS. During the experiments, the reactor and the cone were insulated using an oven. A nickel skimmer with a 1.25 mm diameter aperture was located about 15 mm downstream from the sampling nozzle (50 μm tip orifice). The formed molecular beam was then measured by the SVUV-PI-MBMS, which enables the measurement of peroxides, especially those with three to five oxygen atoms. The Hefei experiments were performed with an initial MCH mole fraction of 0.01, equivalence ratio of 1.0, and temperature of 500–800 K.

3. Kinetic model and simulation method

The MCH mechanism in this study was built on top of a previously developed *n*-heptane oxidation mechanism [32]. The high-temperature chemistry of MCH incorporates the high-temperature mechanism developed by Wang et al. [9], with the addition of extra reaction classes taken from Weber et al. [13]. The low-temperature mechanism was developed referring to Weber et al.'s mechanism and to the low-temperature reaction classes proposed by Sarathy et al. for *n*- and *iso*-alkanes [33]. The low-temperature oxidation scheme was extended to include the "alternative isomerization", concerted elimination, and third O_2 addition pathways for OOQOOH radicals [28], as shown in Scheme 1. The "alternative isomerization" pathway involves an alternative

isomerization step in which the OOQOOH internally abstracts an H-atom that is not α to the OOH group. The reaction class numbers in Scheme 1 are taken from [33]. Additionally, rate constants have been updated to incorporate recently published information [19,20,26], and thermodynamic data were estimated from the group additivity method implemented in THERM [34] using the updated group values by Burke et al. [29]. Lastly, a knowledge-based approach to reduce the complexity of the low-temperature chemistry of MCH was investigated. Details of the reaction mechanism and the sources of rate parameters for MCH pyrolysis are provided in Table S1 of Supplementary Material-1 (SM-1).

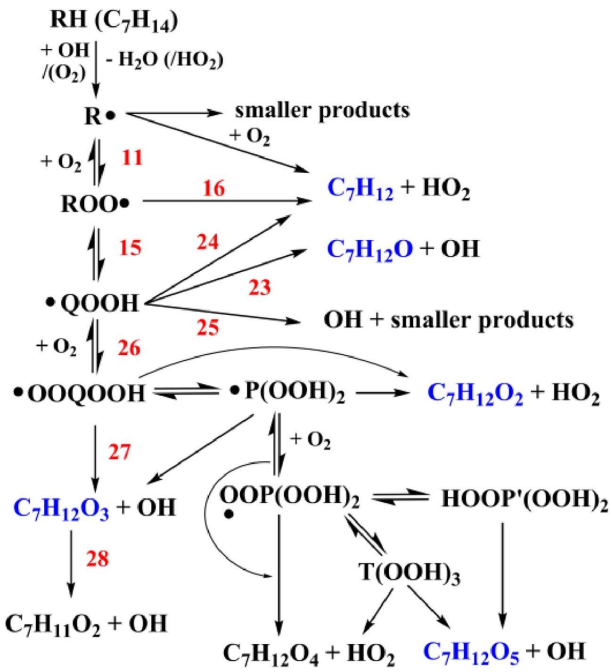

Scheme 1. General reaction mechanism of MCH oxidation. Species with molecular formula detected in this work are highlighted in blue. The numbers on arrows denote the reaction class discussed in this text.

Previous studies have shown that the sterically hindered cyclic structure of cycloalkanes greatly affects the low-temperature oxidation [19,20]. Ring strain energy and frozen rotors imposed by the cyclic structure lead to remarkable deviations from rate constants estimated by analogy to linear alkanes. Investigations are needed to explore rate rules for individual cyclic alkane's low-temperature oxidation. Xing et al. [19,20] recently studied the low-temperature oxidation chemistry of three typical MCH radicals (CYCHEXCH2, MCHR1, MCHR2) using theoretical calculations. They provided temperature and pressure dependent rate constants involving the radicals, CYCHEXCH2 ( ), MCHR1 ( ) and MCHR2 ( ), for the following reaction classes: 11, 15, 16, 23, 24, and 25 (see Scheme 1). Hence, these rates were adopted in the proposed reaction mechanism. The cyclohexane rate constants computed by Fernandes et al. [26] were used for R + O_2 and subsequent reactions involving the ring in MCH for MCHR3 ( ) and MCHR4 ( ). Adjustments were required for class 15 [alkylperoxy (ROO) ↔ hydroperoxyalkyl (QOOH)] isomerization reactions due the presence of a methyl branch in MCH compared to cyclohexane. The activation energy was reduced by 2 kcal mol^{-1} for reactions involving a tertiary CH based on Evans-Polanyi correlation with a secondary CH, and the degeneracy of hydrogen atoms were corrected when necessary following symmetry differences.

The MCH reaction network for ROO ↔ QOOH isomerization becomes increasingly complex due to the large number of reaction pathways. Typically, isomerization pathways proceeding via 5, 6, 7, and 8 membered-ring transition states should be included. However, upon comparison of the rate constants for the isomerization pathways of ROO radicals of MCH, 6 membered-ring transition states were found to have considerably larger rate constants (see Fig. S1 in Section 1 of SM-2). To reduce the complexity of the low-temperature chemistry, only 6 membered-ring isomerizations and isomerizations leading to products detected in the Nancy JSR-2 experiment were included. Tests were conducted to verify that neglecting the non-six membered isomerization pathways has limited effect on ignition delay times (IDT) across a wide range of temperatures and pressures (Figure S2 in Section 1 of SM-2).

The second O_2 addition to QOOH intermediates (class 26) leads to low-temperature chain branching. Here, the second O_2 addition rate coefficients are identical to those of the first O_2 addition, however the pre-exponential factors were divided by 2 based on the findings of Goldsmith et al. [35]. Following the second O_2 addition, keto-hydroperoxide (KHP) and an OH radical are formed following an OOQOOH isomerization step. In the previously developed low-temperature MCH mechanism [13], rates were obtained using estimations based on acyclic analogues rates. As stated previously, this may be inaccurate. In this mechanism, the rate coefficients for isomerizations of OOQOOH to KHP + OH were assigned using the same rate coefficients as those of the isomerizations of ROO to QOOH. However, due to weakened CH bond strength (abstracted hydrogen is bound at the α-site to the hydroperoxy group), an additional reduction of 3 kcal mol^{-1}, as proposed by Sarathy et al. [33], was implemented for isomerization not involving the cyclic ring. Isomerizations involving the cyclic ring need to be further scrutinized as the second added O_2 must be in an appropriate position to enable an internal H-abstraction transition state (both groups axially positioned), or else this will lead to significant ring strain. The published literature on this subject is minimal, so an attempt has been made to estimate rates. Again, the same rate coefficients as those of isomerization of ROO to QOOH were used; however, in consideration of the potential ring strain, the activation energy was reduced by 2 kcal mol^{-1}, instead of 3 kcal mol^{-1}.

In most alkane oxidation mechanisms [33], the hydroperoxyalkylperoxy radical (OOQOOH) only undergoes internal H-atom migration from the weakest hydrogen at the alpha site to the peroxy group, producing a KHP and an OH radical. However, recent studies involving acyclic and cyclic alkanes, have shown that the intramolecular migration of H-atoms from other carbon sites in OOQOOH radicals could be competitive [36]. Yang et al. [37] stated that the formation of a KHP for cyclohexane is "sterically unlikely as the axial hydroperoxy group stands in the way and prevents the equatorial hydrogen from being reached by the peroxy group". With this path closed, it is likely that the chain branching will proceed via an "alternative isomerization" pathway to produce dihydroperoxyalkyl radicals ($P(OOH)_2$). Secondly, following the first O_2 addition to a tertiary site (e.g., MCHR1), ROO ↔ QOOH, and subsequent second O_2 addition, there will be no α-hydrogen present for abstraction. To continue with chain branching pathways, the suggested "alternative isomerization" pathway seems probable. Thus, "alternative isomerization" of OOQOOH and subsequent reaction pathways of $P(OOH)_2$ species have been included in this mechanism (see Scheme 1). This is in accord with the experimental measurements of intermediates which are likely to have formed following the reaction network of the "alternative isomerization" of OOQOOH to $P(OOH)_2$, and the third sequential O_2 addition of $P(OOH)_2$ in the literature [28] and also in this work (see Section 4). Analogies and estimations have been used to formulate rate coefficients of all added reactions due to the limited published data, see SM-1.

Further reduction to the mechanism was applied by analyzing whether the second O_2 addition to QOOH and third O_2 addition to $P(OOH)_2$ were major pathways. For example, upon the formation of a QOOH species, there are three reaction pathways: QOOH + O_2 = OOQOOH or QOOH = cyclic ether + OH or QOOH = olefin + HO_2. The sources for the rate constants of these three reactions are from Xing et al.[19], [20] and Fernandes et al. [26]. The analysis shows that the unimolecular reactions of β-QOOH/β-$P(OOH)_2$ to cyclic ether and OH were more favorable than the O_2 addition pathways (see Fig. S3 in Section 1 of SM-2). Here, β-QOOH/β-$P(OOH)_2$ denotes the QOOH/$P(OOH)_2$ that the radical site is β to the nearest –OOH group. Thus, in this work, the O_2 additions to β-QOOH and β-$P(OOH)_2$ were not included. In addition, certain intermediates were lumped to reduce the complexity of the reaction scheme. Details of the lumped species are presented in Table S2 of SM-1. Developing kinetic mechanisms is a time-consuming task and reducing the reaction pathways, wherever appropriate, during the development can reduce the complexity and size of the mechanism. The inclusion of all theoretically possible reaction pathways is cumbersome, especially when the pathways do not play a significant effect. The present knowledge-based approach could prove invaluable when developing kinetic mechanism of fuels that produce many radical isomers.

JSR simulations were performed by CHEMKIN-PRO [38] using the perfectly stirred reactor module (transient solver with an end time of 30 s). In certain simulations above 1000 K, the transient solver was hard to converge, so the steady state solver was adopted. The RCM IDT of MCH was simulated using the closed batch reactor and the supplied volume profiles [13,14].

4. Results and discussion

The low-temperature oxidation chemistry of MCH is more complex than its pyrolysis and oxidation at high temperature. Elucidating the intermediate species pool at low temperatures is the first step to developing comprehensive reaction mechanisms and to examine kinetic modeling predictions. In the SVUV-PI-MBMS analysis, the mass spectrum of MCH oxidation in JSR-3 at 570 K was measured at 10.5 eV, corresponding to a fuel conversion of ~30%, as shown in Figure S4 in Section 2 of SM-2. The major intermediates at the early stage of oxidation are oxygenated compounds, which include C_1-C_5 species with one to two oxygen atoms (CH_3OOH, C_2H_4O, C_3H_6O, C_3H_8O, C_4H_6O, C_4H_8O, C_5H_8O, and $C_5H_{10}O$) and C_7 species with zero to five oxygen atoms (C_7H_{12}, $C_7H_{10}O$, $C_7H_{12}O$, $C_7H_{10}O_2$, $C_7H_{12}O_2$, $C_7H_{14}O_2$, $C_7H_{12}O_3$, $C_7H_{10}O_4$, and $C_7H_{12}O_5$). In the Nancy JSR-2 experiment, the oxidation intermediates from C_1-C_7 were also measured. The major component for C_2H_4O is acetaldehyde, while oxirane is a minor component. Acrolein is the only isomer for C_3H_4O while both methacrolein and methyl vinyl ketone were observed for C_4H_6O. For C_3H_6O, C_4H_8O and $C_5H_{10}O$, both aldehyde and ketone compounds were measured, e.g., propanal and acetone for C_3H_6O, butanal and butanone for C_4H_8O, and pentanal and 2-pentanone for $C_5H_{10}O$. Furthermore, two kinds of intermediates with the same carbon atoms of MCH were measured, i.e., C_7H_{12} and $C_7H_{12}O$. The C_7H_{12} intermediates were detected as methylcyclohexenes. 1-methyl-cyclohexene was separated from the GC analysis while other isomers were not separated and their mole fractions were summed together. For $C_7H_{12}O$, eight isomers were observed, including MCH-aldehyde (cyclohexanecarboxaldehyde), MCH-ketone (2-methyl-cyclohexanone and 3-methyl-cyclohexanone), and MCH-cyclic ethers with three and five membered rings (1-oxaspiro[2,5]octane, 1-methyl,7-oxabicyclo[2.2.1]heptane, 1-methyl,7-oxabicyclo[4.1.0]heptane). The four membered ring MCH-cyclic ether (e.g., 1-methyl,7-oxabicyclo[3.1.1]heptane) was not detected from the experiment due to its instability. The GC analysis measured its two isomerization products: 6-heptenone and 5-methyl,5-hexenal. The structure of these $C_7H_{12}O$ intermediates are presented in Table S1 in Section 2 of SM-2. The

separation and quantification of these $C_7H_{12}O$ intermediates are valuable to understand the first O_2 addition process of MCH, especially to elucidate the branching ratios of unimolecular decomposition and O_2 addition to QOOH radical.

The mass peaks corresponding to C_7H_{12} and $C_7H_{12}O$ were also observed from the SVUV-PI-MBMS experiment. In addition, several highly oxygenated intermediates were detected during MCH oxidation. In the previous work by Wang et al. [28], the highly oxygenated intermediates were measured by atmospheric pressure chemical ionization orbitrap mass spectrometer. Compared to this previous work, new data of the signal profiles of the C_7 intermediates are presented in Fig. 1. These data are valuable to validate the model. We note that the mole fraction of MCH was quantified while that of the C7 intermediates was not evaluated due to unknown photoionization cross sections. Similar to a previous comprehensive SVUV-PI-MBMS investigation for hydrocarbons and oxygenated compounds [28], $C_7H_{12}O_3$, $C_7H_{10}O_4$, and $C_7H_{12}O_5$, correspond to intermediates with one –OOH (e.g., KHP/hydroperoxy cyclic ether), one –OOH (e.g., diketo-hydroperoxide/keto-hydroperoxy cyclic ether), and two –OOHs (e.g., keto-dihydroperoxide/dihydroperoxy cyclic ether), respectively. The detection of $C_7H_{12}O_5$ is further evidence of second O_2 addition to a QOOH radical, "alternative isomerization" of OOQOOH to $P(OOH)_2$ radical, and a third sequential O_2 addition, as shown in Scheme 1. The SVUV-PI-MBMS experiment detected four other intermediates: $C_7H_{14}O_2$, $C_7H_{12}O_2$, $C_7H_{10}O_2$, and $C_7H_{10}O$. These species can be produced via secondary reactions. The $C_7H_{14}O_2$ intermediates could be methylcyclohexyl peroxides that are produced from the cross combination of RO_2 with HO_2 radicals (e.g., $RO_2 + HO_2 = ROOH + O_2$). The $C_7H_{10}O_2$ species could be produced from the OH radical assisted water elimination of KHP [39]. Based on the recent study of n-heptane [40] and theoretical calculation for the H-atom abstraction of KHP from *n*-pentane oxidation [39], the $C_7H_{10}O$ intermediates could be formed from the H-atom abstraction of KHP and the subsequent decomposition of KHP radicals via the loss of HO_2 radical.

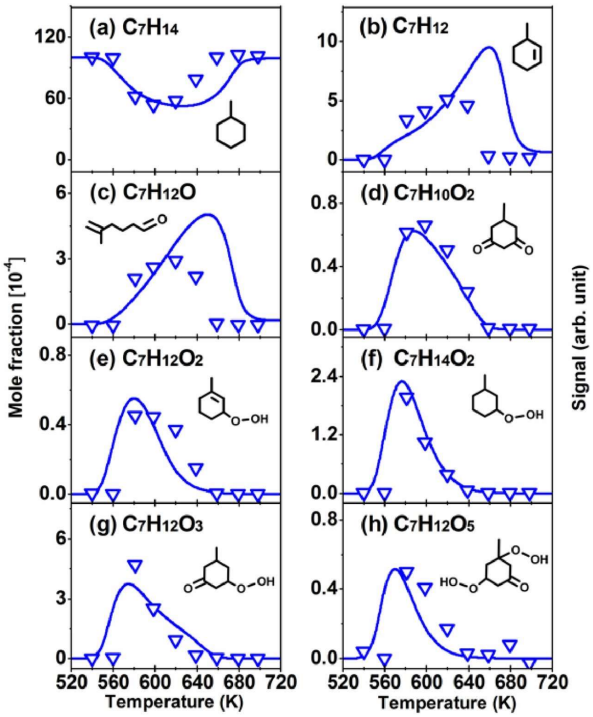

Figure 1. Symbols are SVUV-PI-MBMS mole fraction of MCH and signal profiles of C_7 intermediates, while lines are model prediction by the tuned kinetic model (refer to text). The represented structure of these intermediates are shown.

The simulation for the low-temperature oxidation of MCH in Nancy JSR-2 and the RCM IDT of MCH by Mittal and Sung [14], and Weber et al. [13] is presented in Figure 2. Although we updated the rate constants using theoretical calculations and estimated the rate constants for some reactions from literature knowledge and experience, the model prediction in dashed lines for MCH profiles in JSR is more reactive than the measurement (Figure 2a). Additionally, the predicted IDTs are shorter than the measurements, especially in the negative-temperature coefficient zone.

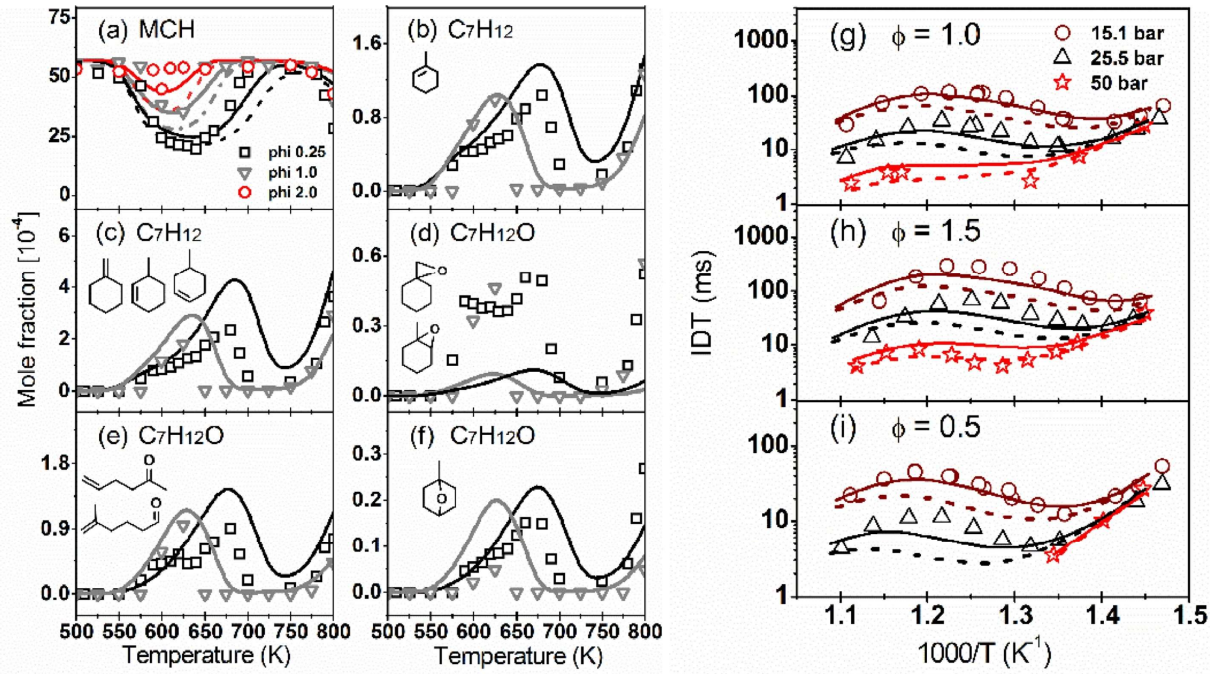

Figure 2. (a–f), experimental and predicted mole fractions of MCH and its initial oxidation products in Nancy JSR-2, φ = 0.25, 1.0, and 2.0. (g–i), experimental and simulated IDT of MCH in RCM [13], [14]. Pressures of 15.1, 25.5 and 50 bar, MCH/O_2/N_2/AR mixture, φ = 0.5, 1.0, and 1.5. Symbols represent experimental measurements. Dashed and solid lines represent the un-tuned and tuned model predictions respectively. The experimental and simulated profiles of C_7H_{12} in Figure 2c are summed mole fraction of the molecule shown in the figure. The experimental profiles of $C_7H_{12}O$ in Figure 2d and e are summed mole fraction of the molecule shown in the figures, while that for simulation is the summation of all the isomers with similar structures.

To resolve the aforementioned discrepancies, the model was tuned to improve the fitting to the experimental data. This tentative tuning is based on the sensitivity analysis, and refers to the work of Mohamed et al. [41]. The temperature sensitivity analysis of MCH ignition delay time at 25.5 bar and equivalence ratios of 1.0 and 0.5 was carried out (Figure S5 in Section 2 of SM-2). The initial temperature is 830 K at the NTC zone, where the largest deviation between simulation and experiment was observed. The sensitivity coefficient at the time just before ignition occurs was adopted for analysis. Apart from the reactions related to MCH (e.g., MCH + OH and MCH + HO_2) and reactions of H_2O_2 in the base chemistry, the reactions related to the formation of HO_2 and OH radicals have large effect on the ignition. For example, concerted elimination of ROO radicals that promote HO_2 production has a large negative effect on the ignition. In contrast, the reactions promoting the OH radical formation, e.g., the isomerization of ROO to QOOH and the second O_2 addition to QOOH, have large positive effect on ignition delay time. The positive sensitivity value increases the fuel reactivity and shortens the ignition delay time, and vice versa. The rate constants selected for tuning are those initially estimated based on analogies, and therefore have

larger uncertainties. We did not tune rate constants that were assigned from previous theoretical calculations.

Details of the tuning are as follows: (1) The pre-exponential term was increased by a factor of 4 for $RO_2 + HO_2 = ROOH + O_2$; (2) The pre-exponential term of second and third O_2 additions was reduced by a factor of 2 (i.e., the rate is 4x slower than $R + O_2 = RO_2$); (3) an activation energy of 41.6 kcal mol^{-1} was used for KHP decomposition, which is the same value as that used in Weber et al's [13] MCH kinetic model. The solid lines in Fig. 2 represent the tuned model predictions. An improvement is evident for both JSR and RCM IDT simulations. However, there is still a discrepancy for the IDT under some conditions. The initial oxidation products of MCH in Nancy JSR-2 measurements, e.g., alkenes and cyclic ethers, are satisfactorily predicted by the tuned model. We note that the simulated mole fraction for the three-membered ring cyclic ethers (Fig. 2d) and the unsaturated keto/aldehyde compounds (Figure 2e) are a summation of all isomers. It is interesting to note the high concentration of three-membered ring cyclic ethers, which is comparable to that of the four-membered ring cyclic ethers (i.e., Figure 2d and e). However, the kinetic analysis reveals that pathways to three-membered ring cyclic ethers are unfavorable. The under-prediction of these intermediates is probably due to deficiencies in the kinetic model, and more study for their reaction mechanism is necessary.

The purpose of the present model development was not presenting a perfectly tuned model. More experimental data, for MCH and other cycloalkanes, is needed to tune the model and establish reasonable rate rules for cycloalkane auto-ignition. In addition, the kinetic information on the low-temperature reaction pathways of cycloalkanes and their rate constants are still lacking. In any case, the kinetic model developed is this work could be used as a basis for further model development (SM-3). The glossary and SMILES notation of the species in MCH sub-mechanism are shown in SM-4.

The tuned model was also used to predict the MCH oxidation in Hefei JSR-3. As shown in Fig. 1, the model captures the consumption of MCH before the NTC. However, MCH consumption is over-predicted in the NTC regime. The model also captures the signal profiles of the initial C_7 intermediates, except that C_7H_{12} and $C_7H_{12}O$ in the NTC zone.

The reaction pathway for MCH consumption was analyzed at 600 K, $\varphi = 1.0$ in Nancy JSR-2. As shown in Figure S6 in Section 2 of SM-2, MCH is consumed by OH radical via H-atom abstraction and several MCH radicals are formed. At 600 K, these radicals react with O_2 to form ROO radicals. Three reaction class participates in the subsequent reaction of ROO, i.e., concerted elimination to form C_7H_{12} olefin and HO_2 radical, intramolecular isomerization to form QOOH radicals, and bimolecular reactions with HO_2 to form $C_7H_{13}OOH$ peroxide. Similar to MCH radicals, the dominant reaction for the QOOH radicals is O_2 addition to the radical site leading to OOQOOH radicals. The OOQOOH radicals are consumed by concerted elimination to $C_7H_{12}O_2$ olefinic hydroperoxides, decomposition to $C_7H_{12}O_3$ keto-hydroperoxides, and further isomerization to $P(OOH)_2$ radicals. A specific example for the reaction pathways of the ROO radical generated from MCHR3 () are presented in Figure 3. The various isomers of C_7H_{12}, $C_7H_{12}O$, $C_7H_{12}O_2$, and $C_7H_{12}O_3$ are produced. For the $P(OOH)_2$ radical, its decomposition forms another isomer of $C_7H_{12}O_3$ while its third O_2 addition leads to $C_7H_{12}O_5$ intermediates. All these intermediates have been detected from the SVUV-PI-MBMS experiment. The represented structure of these intermediates are also presented in Figure 1

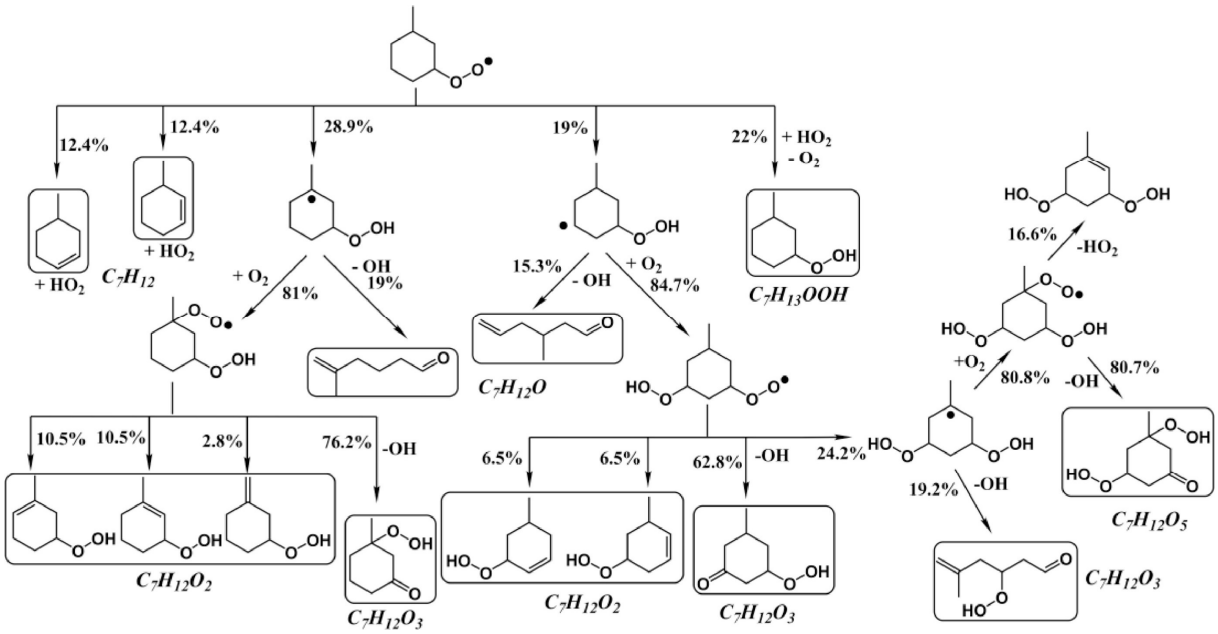

Figure 3. Reaction pathway analysis of the ROO radical produced from MCHR3 (•⬡) in MCH JSR oxidation in Nancy JSR-2. The equivalence ratio is 1.0 and temperature is 600 K the m/z of the boxed species is detected from the SVUV-PIMS experiment.

The discussion of the pyrolysis and high-temperature oxidation chemistry is presented in Section 3 and Figure S7 of SM-2. In addition, the flow reactor pyrolysis of MCH at various pressures in the literature [9] were also simulated. The prediction for MCH conversion and the formation of intermediates and final products is also satisfactory (Figures S8 and S9 in Section 3 of SM-2). The GC measured mole fractions of MCH pyrolysis and oxidation are presented in SM-5.

5. Conclusions

In this work, we investigated the combustion chemistry of MCH by measuring species distribution from JSR pyrolysis and oxidation. Initial hydrocarbon and oxygenated intermediates, indicative of the first, second, and third O_2 addition reactions in MCH low-temperature oxidation, were measured by GC and SVUV-PI-MBMS analysis. The measurements of dozens of species are valuable to examine kinetic models for MCH gas-phase oxidation and pyrolysis. A preliminary kinetic model for MCH pyrolysis and oxidation has been built based on literature studies. Specifically, rate constants of key reactions of MCH low-temperature oxidation were taken from theoretical calculations, thermodynamic data were estimated from Benson group additivity with implemented new group values, and "alternative isomerization" of OOQOOH and a third sequential O_2 addition reaction network were included on the basis of the experimental observation. However, the model's prediction for MCH JSR oxidation and RCM IDT was faster compared to the experimental measurements, which indicates unreasonable branching ratios in low-temperature pathways governing OH and HO_2 radical concentrations. A tentative tuning of the rate constants for three reactions, initially estimated based on analogies, resulted in a better prediction of the measurements. Further tuning of the model with systematic rate rules can be developed when additional experimental measurements and theoretical calculations of cycloalkane auto-oxidation are made available. It is recommended that theoretical studies focus on the kinetics of MCH + HO_2, second and third O_2 addition reactions, KHP decomposition, and alternative isomerizations. Additional experimental data in JSR and shock tube ignition delay times at high pressures and low temperatures are necessary to improve the model's performance.

Acknowledgments

This work was supported by: King Abdullah University of Science and Technology (KAUST), Office of Sponsored Research (OSR) under Award No. OSR-2016-CRG5-3022, and Saudi Aramco under the FUELCOM program. European Commission ("Clean ICE" ERC Advanced Research Grant, 2008–2013) is thanked for supporting Nancy experiments.

Supplementary materials

- Supplementary tables
- Supplementary figures
- Detailed kinetic model
- Species nomenclature
- Experimental data

References

[1] S. Saxena, I.D. Bedoya, Prog. Energy Combust. Sci., 39 (2013), pp. 457-488
[2] W.J. Pitz, C.J. Mueller, Prog. Energy Combust. Sci., 37 (2011), pp. 330-350
[3] S.M. Sarathy, A. Farooq, G.T. Kalghatgi, Prog. Energy Combust. Sci., 65 (2018), pp. 67-108
[4] L.M. Shafer, R.C. Striebich, J. Gomach, T. Edwards AIAA (2006), 2006-7972
[5] Zhang H.R., E.G. Eddings, A.F. Sarofim, Environ. Sci. Technol., 42 (2008), pp. 5615-5621
[6] M.J. Al Rashidi, M. Mehl, W.J. Pitz, S. Mohamed, S.M. Sarathy, Combust. Flame, 183 (2017), pp. 358-371
[7] M.J. Al Rashidi, J.C. Mármol, C. Banyon, et al., Combust. Flame, 183 (2017), pp. 372-385
[8] Wang Z., Cheng Z., Yuan W., et al., Combust. Flame, 159 (2012), pp. 2243-2253
[9] Wang Z., Ye L., Yuan W., et al., Combust. Flame, 161 (2014), pp. 84-100
[10] Wang Z., Zhao L., Wang Y., et al., Combust. Flame, 162 (2015), pp. 2873-2892
[11] R. Bounaceur, V. Burklé-Vitzthum, P.-M. Marquaire, L. Fusetti, J. Anal. Appl. Pyrolysis, 103 (2013), pp. 240-254
[12] S.A. Skeen, Yang B., A.W. Jasper, W.J. Pitz, N. Hansen, Energy Fuels, 25 (2011), pp. 5611-5625
[13] B.W. Weber, W.J. Pitz, M. Mehl, E.J. Silke, A.C. Davis, Sung C.-J., Combust. Flame, 161 (2014), pp. 1972-1983
[14] Mittal G., Sung C.-J., Combust. Flame, 156 (2009), pp. 1852-1855
[15] Wu F., A.P. Kelley, C.K. Law, Combust. Flame, 159 (2012), pp. 1417-1425
[16] S. Granata, T. Faravelli, E. Ranzi, Combust. Flame, 132 (2003), pp. 533-544
[17] K. Narayanaswamy, H. Pitsch, P. Pepiot, Combust. Flame, 162 (2015), pp. 1193-1213
[18] Zhang F., Wang Z.D., Wang Z.H., Zhang L.D., Li Y.Y., Qi F., Energy Fuels, 27 (2013), pp. 1679-1687
[19] Xing L., Zhang L., Zhang F., Jiang J., Combust. Flame, 182 (2017), pp. 216-224
[20] Xing L., Zhang F., Zhang L., Proc. Combust. Inst., 36 (2016), pp. 179-186
[21] K. Moshammer, A.W. Jasper, D.M. Popolan-Vaida, et al., J. Phys. Chem. A, 120 (2016), pp. 7890-7901
[22] Qi F., Yang R., Yang B., et al., Rev. Sci. Instrum., 77 (2006), Article 084101
[23] P. Oßwald, H. Güldenberg, K. Kohse-Höinghaus, Yang B., Yuan T., Qi F., Combust. Flame, 158 (2011), pp. 2-15
[24] Yang B., P. Oßwald, Li Y., et al., Combust. Flame, 148 (2007), pp. 198-209
[25] Qi F., Proc. Combust. Inst., 34 (2013), pp. 33-63

[26] R.X. Fernandes, J. Zador, L.E. Jusinski, J.A. Miller, C.A. Taatjes, Phys. Chem. Chem. Phys., 11 (2009), pp. 1320-1327
[27] Wang Z., S.Y. Mohamed, Zhang L., et al., Proc. Combust. Inst., 36 (2017), pp. 373-382
[28] Wang Z., D.M. Popolan-Vaida, Chen B., et al., Proc. Natl. Acad. Sci. USA, 114 (2017), pp. 13102-13107
[29] S.M. Burke, J.M. Simmie, H.J. Curran, J. Phys. Chem. Ref. Data, 44 (2015), Article 013101
[30] Chen B., Wang Z., Wang J.-Y., et al., Fuel (2018), under review
[31] B. Husson, O. Herbinet, P.A. Glaude, S.S. Ahmed, F. Battin-Leclerc, J. Phys. Chem. A, 116 (2012), pp. 5100-5111
[32] Zhang K., C. Banyon, J. Bugler, et al., Combust. Flame, 172 (2016), pp. 116-135
[33] S.M. Sarathy, C.K. Westbrook, M. Mehl, et al., Combust. Flame, 158 (2011), pp. 2338-2357
[34] E.R. Ritter, J.W. Bozzelli, Int. J. Chem. Kinet., 23 (1991), pp. 767-778
[35] C.F. Goldsmith, W.H. Green, S.J. Klippenstein, J. Phys. Chem. A, 116 (2012), pp. 3325-3346
[36] J. Bugler, K.P. Somers, E.J. Silke, H.J. Curran, J. Phys. Chem. A, 119 (2015), pp. 7510-7527
[37] Yang Y., A.L. Boehman, J.M. Simmie, Combust. Flame, 157 (2010), pp. 2369-2379
[38] CHEMKIN-PRO 15112, Reaction Design: San Diego, (2012).
[39] Xing L., Bao J.L., Wang Z., Zhang F., D.G. Truhlar, J. Am. Chem. Soc., 139 (2017), pp. 15821-15835
[40] Wang Z., Chen B., K. Moshammer, et al., Combust. Flame, 187 (2018), pp. 199-216
[41] S.Y. Mohamed, Cai L., F. Khaled, et al., J. Phys. Chem. A, 120 (2016), pp. 2201-2217